Targeting Notch, a key pathway for ovarian cancer stem cells, sensitizes tumors to platinum therapy

Shannon M. McAuliffe[a,1], Stefanie L. Morgan[a,1], Gregory A. Wyant[a,2], Lieu T. Tran[a,2], Katherine W. Muto[a,2], Yu Sarah Chen[a,2], Kenneth T. Chin[a], Justin C. Partridge[a], Barish B. Poole[a], Kuang-Hung Cheng[a], John Daggett, Jr.[a], Kristen Cullen[b], Emily Kantoff[c], Kathleen Hasselbatt[d], Julia Berkowitz[a], Michael G. Muto[c,d], Ross S. Berkowitz[c,d], Jon C. Aster[a], Ursula A. Matulonis[c], and Daniela M. Dinulescu[a,3]

Departments of [a]Pathology and [d]Obstetrics, Gynecology and Reproductive Biology, Brigham and Women's Hospital, Harvard Medical School, Boston, MA 02115; [b]Cell Signaling Technology, Danvers, MA 01923; and [c]Department of Medical Oncology, Dana-Farber Cancer Institute, Boston, MA 02115

Edited* by Patricia K. Donahoe, Massachusetts General Hospital, Boston, MA, and approved August 29, 2012 (received for review April 17, 2012)

Chemoresistance to platinum therapy is a major obstacle that needs to be overcome in the treatment of ovarian cancer patients. The high rates and patterns of therapeutic failure seen in patients are consistent with a steady accumulation of drug-resistant cancer stem cells (CSCs). This study demonstrates that the Notch signaling pathway and Notch3 in particular are critical for the regulation of CSCs and tumor resistance to platinum. We show that Notch3 overexpression in tumor cells results in expansion of CSCs and increased platinum chemoresistance. In contrast, γ-secretase inhibitor (GSI), a Notch pathway inhibitor, depletes CSCs and increases tumor sensitivity to platinum. Similarly, a Notch3 siRNA knockdown increases the response to platinum therapy, further demonstrating that modulation of tumor chemosensitivity by GSI is Notch specific. Most importantly, the cisplatin/GSI combination is the only treatment that effectively eliminates both CSCs and the bulk of tumor cells, indicating that a dual combination targeting both populations is needed for tumor eradication. In addition, we found that the cisplatin/GSI combination therapy has a synergistic cytotoxic effect in Notch-dependent tumor cells by enhancing the DNA-damage response, G_2/M cell-cycle arrest, and apoptosis. Based on these results, we conclude that targeting the Notch pathway could significantly increase tumor sensitivity to platinum therapy. Our study suggests important clinical applications for targeting Notch as part of novel treatment strategies upon diagnosis of ovarian cancer and at recurrence. Both platinum-resistant and platinum-sensitive relapses may benefit from such an approach as clinical data suggest that all relapses after platinum therapy are increasingly platinum resistant.

tumor models | Notch3 expression patterns | isobologram and combination index analysis | platinum-induced DNA damage response | synergistic cytotoxic effects for GSI/cisplatin combination therapy

Ovarian cancer is the fifth leading cause of cancer death in women. Each year in the United States ~22,000 women are diagnosed resulting in over 16,000 deaths annually (1). The high mortality results partially from the nonspecific and commonly misinterpreted symptoms associated with the disease. As a result, more than 70% of patients are diagnosed only after the disease has progressed to a late stage (2). Although standard treatment involving cytoreduction surgery and platinum/paclitaxel therapy can achieve clinical remission independent of disease stage, more than two-thirds of late-stage patients will relapse and develop resistance to the first-line drugs (2, 3). Therefore it is essential to target the mechanisms governing intrinsic and acquired chemoresistance. Improving the current responses to platinum chemotherapy is key not only for achieving a better outcome clinically, including a longer survival, but also for allowing patients to have a better quality of life during treatment.

Most research studies currently are focusing on investigating the key genetic mutations and pathways leading to malignancy for all tumor types, independent of tumor heterogeneity and differences in biology and tumorigenic potential (4–8). Cancer stem cells (CSCs) are thought to be important for both tumor development and chemoresistance to therapy because of their ability to divide indefinitely, contribute to cancer invasion and metastasis through the epithelial–mesenchymal transition program, and survive standard cancer chemotherapies (9–11). Numerous reports support the existence of tumor subpopulations with CSC-like properties in hematological and solid malignancies, including ovarian cancer (12–17). Five-year survival rates for women with newly diagnosed ovarian cancer are dismally low (20–25%) despite the use of conventional platinum-based chemotherapy, with no recent meaningful gains in life expectancy (18–21). Drug-resistant self-renewing CSCs, which evade the anti-cancer effects of systemic chemotherapy, are a potential reason for the observation that most patients with advanced ovarian cancer will recur at some point post platinum-based chemotherapy and develop multidrug resistance (MDR). It is well established that CSCs have important similarities with normal stem cells: they both express high levels of efflux transporters and are very efficient in repairing DNA damage. Consequently, these stem-cell characteristics render CSCs resistant to conventional chemotherapy. Current therapies target the bulk of the rapidly dividing, non-CSC tumor cells, thus reducing tumor mass but leaving behind drug-resistant CSCs. Successful tumor elimination requires a combination therapy that affects both differentiated cancer cells and the CSC population (22).

Increasing evidence suggests that elucidating the genetic mutations and pathways that specifically target CSCs is critical. Several cellular signaling pathways, including Notch, WNT/β-catenin, PTEN, FGF, IGF1, TGF-β, and Bmi-1, which have been implicated in regulating self-renewal and cell-fate determination in normal somatic stem cells, also are mutated in human cancers (5–12). For example, Notch signaling, which controls the cell fate determination, survival, proliferation, and maintenance of somatic stem cells, has also been proposed to have a key role in the function of CSCs in a variety of cancers. In ovarian cancer, Notch3 signaling is believed to play a critical role: Notch3 overexpression is found in more than 20% of ovarian serous adenocarcinomas and is correlated with particularly aggressive tumors that have a poor prognosis (23–25). Signaling of the Notch pathway is initiated by the binding of Notch ligands (Jagged and Delta) to Notch receptors. This in turn activates the Notch signaling cascade (HES and other downstream effectors) by releasing the intracellular domain of the Notch re-

Author contributions: S.M.M., S.L.M., G.A.W., L.T.T., Y.S.C., K.T.C., K.-H.C., J.D., J.C.A., and D.M.D. designed research; S.M.M., S.L.M., G.A.W., L.T.T., K.W.M., Y.S.C., K.T.C., J.C.P., B.B.P., K.-H.C., J.D., and J.B. performed research; K.C., E.K., K.H., M.G.M., R.S.B., J.C.A., and U.A.M. contributed new reagents/analytic tools; S.M.M., S.L.M., G.A.W., L.T.T., K.W.M., Y.S.C., K.T.C., J.C.P., B.B.P., K.-H.C., J.D., E.K., K.H., and D.M.D. analyzed data; and S.M.M., S.L.M., G.A.W., L.T.T., K.W.M., Y.S.C., and D.M.D. wrote the paper.

The authors declare no conflict of interest.

*This Direct Submission article had a prearranged editor.

[1]S.M.M. and S.L.M. contributed equally to this work.

[2]G.A.W., L.T.T., K.W.M., and Y.S.C. contributed equally to this work.

[3]To whom correspondence should be addressed. E-mail: DDinulescu@rics.bwh.harvard.edu.

See Author Summary on page 17325 (volume 109, number 43).

This article contains supporting information online at www.pnas.org/lookup/suppl/doi:10.1073/pnas.1206400109/-/DCSupplemental.

ceptor (NICD) through a cascade of proteolytic cleavages mediated in part by γ-secretase.

In this study we sought to explore the involvement of the Notch pathway in the regulation of CSCs. In addition, we determined the efficacy of a Notch pathway inhibitor, γ-secretase inhibitor 1 (GSI), in both murine models and human cell lines in vitro and in vivo and found that it synergized with standard platinum therapy in ovarian cancer. The importance of the Notch pathway, and especially Notch3, in CSC regulation suggests that GSI plays a critical role in decreasing CSCs and, as a result, it reduces chemoresistance and improves the therapeutic response to platinum treatment. In addition, inhibition of Notch3 activity with either siRNAs or GSI sensitizes ovarian cancer cells to cisplatin (CDDP) in tumor cell lines and patient samples exhibiting high levels of Notch3 expression but not in lines where Notch3 is absent. Moreover, we found that Notch pathway inhibitors synergize with CDDP by enhancing the DNA-damage response and cell death induced by platinum. Our results show that key pathways, such as Notch signaling, play an important role in the maintenance of CSCs and platinum chemoresistance and suggest an important clinical application of Notch pathway inhibitors in ovarian cancer therapy.

Results

CSCs Are Important Targets for Overcoming Resistance to Platinum Therapy. Side population (SP) cells, isolated based on their ability to efflux the Hoechst 33342 fluorescent dye, have been shown to be an enriched source of cancer stem and progenitor cells in hematopoietic and several solid malignancies, including ovarian cancer (12–17). Using animal models (26) and human tumors and ascites, we have further characterized SP cells that display characteristics consistent with CSCs or early progenitors (12). We have generated specific molecular profiles of SP cells isolated from ovarian tumors and demonstrated that SP are indeed enriched for ovarian CSCs based on their gene transcriptional profile, key stem-cell surface markers (CD44, CD24, c-kit, CD133, and ALDH1), overexpression of multidrug transporters (ABCG2, ABCB5, and MDR1), self renewal and differentiation properties, and increased tumor-initiating capacity. Furthermore, we have found that ovarian CSCs are resistant to platinum therapy, suggesting that they contribute to intrinsic and acquired platinum chemoresistance in patients.

We identified SP cells enriched for ovarian CSCs in murine cell lines (4306 and 4412) isolated from the cre-activated conditional LSL-K-ras$^{G12D/+}$/Pten$^{loxP/loxP}$ genetically engineered murine model (GEMM) of ovarian cancer (26), as well as in established human lines (OVCAR5) and patient samples (ASC05) (Fig. 1*A*). SP is a reliable marker for the identification of cells enriched for CSCs in both mouse and human samples: the average SP percent in murine 4306 cells is 6.2% (n = 25 FACS experiments, range 1.33–19.5), 1.8% in murine 4412 cells (n = 8 FACS experiments, range 0.4–3.2), and 10.49% in human OVCAR5 cells (n = 5 FACS experiments, range 4.04–22.6), respectively. Our studies demonstrate that ovarian cancer SP cells are more tumorigenic than non-SP (NSP) cells in vivo (Fig. 1*B*), are able to divide indefinitely, and give rise to cobblestone-like epithelial colonies consisting of both SP and NSP cells, whereas NSP cells senesce after 1–2 wk (Fig. 1*C*). In addition, when treated with a wide range of CDDP concentrations (0–80 μM), SP cells are significantly more resistant than NSP cells at concentrations ranging from 2.5 to 40 μM in both murine 4306 and human OVCAR5 cells ($P < 0.05$) (Fig. 1*D*). SP cells were significantly more resistant than NSP cells at individual CDDP doses and showed an increased IC_{50} in response to CDDP as compared with NSP in both lines (a 3.7-fold increase in 4306 cells and a 1.9-fold increase in OVCAR5 cells) (Fig. 1*D*). We also found increased tumor-initiating capacity for SP cells in tumor xenograft studies in vivo using a limiting dilution method to inject sorted SP cells and NSP cells subcutaneously (s.c.) or intraperitoneally (i.p.) into SCID mice (Fig. S1*A*). Injection of as few as 1,000 SP cells resulted in tumor growth in 50% (3/6) of mice, whereas no tumor growth was observed for the same number of

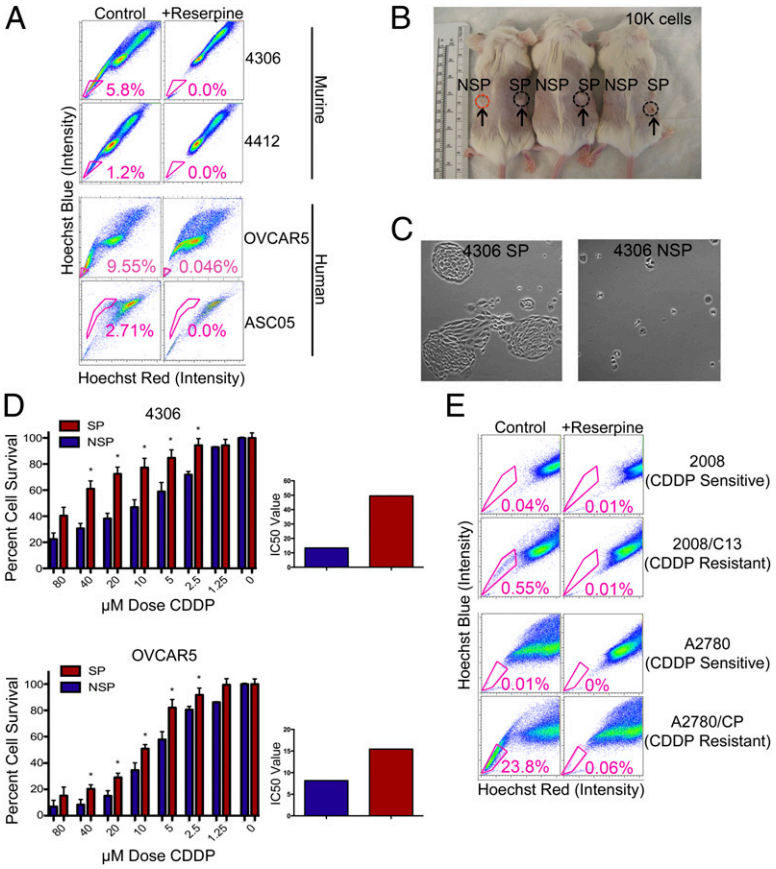

Fig. 1. Identification and characterization of SP cells in ovarian cancer cell lines. (*A*) K-ras/Pten (4306 and 4412) murine lines and human (OVCAR5) and primary patient (ASC05) lines were labeled with Hoechst 33342 dye and analyzed by flow cytometry before and after treatment with reserpine. (*B*) 4306 cells were sorted for SP and NSP, and 10^4 cells were injected into the right and left flanks of SCID mice. Within 9 wk, more tumors were generated from SP xenografts (in three of three mice) than from NSP xenografts (in one of three mice). (*C*) 4306 SP and NSP cells were cultured and photographed at the same magnification. 4306 SP cells formed tight colonies after 4 d in culture, whereas NSP cells were scattered and did not proliferate. (*D*) 4306 and OVCAR5 SP cells are more chemoresistant than NSP cells (*$P < 0.05$), as shown by MTT assay. SP cells were significantly more resistant than NSP cells at individual platinum (CDDP) doses and showed an increased IC_{50} in response to CDDP as compared with NSP in both lines (a 3.7-fold increase in 4306 cells and a 1.9-fold increase in OVCAR5 cells). *$P < 0.05$. (*E*) CDDP-resistant lines 2008/C13 and A2780/CP showed a high increase in CSC percentage (0.55% and 23.8%) as compared with their respective CDDP-sensitive lines (0.04% and 0.01%).

sorted NSP cells. In addition, both murine (4306) and human (OVCAR5) SP cells expressing CD44 ($CD44^+$) exhibited stem-cell characteristics of shorter tumor-free intervals in vivo after limiting dilution (Fig. S1*A*).

In further support of the CSC hypothesis, SP analysis of established CDDP-sensitive (2008 and A2780) and -resistant (2008/C13 and A2780/CP) ovarian cancer lines, provided by Stephen Howell (University of California at San Diego, La Jolla, CA), showed a marked increase in the SP percent in the CDDP-resistant lines compared with their CDDP-sensitive counterparts (0.04% in 2008 increasing to 0.55% in 2008/C13 and 0.01% in A2780 increasing to 23.8% in A2780/CP, respectively) (Fig. 1*E*). Our results suggest that CSCs are greatly expanded during the acquisition of CDDP resistance. These data further prove that conventional treatments target the bulk of cancer cells but leave behind CSCs, which maintain and propagate an increasingly chemoresistant tumor.

Notch Signaling Pathway and Notch3 Specifically Are Critical for the Regulation of CSCs and Platinum Chemoresistance. Given that SP contains a heterogeneous population of cells, including CSCs and progenitors (12), we sought to enrich and purify CSCs further by identifying key cell-surface markers. Thus, we identified and validated a functional and molecular profile of ovarian CSCs (Fig. 2). For this purpose we sorted SP and NSP cells by FACS from murine models for ovarian carcinoma and human cell lines. Sorted SP and NSP cells from murine K-ras/Pten tumor lines (4306) and human tumor lines (OVCAR5 and A2780) were subjected to high-throughput quantitative real-time PCR analysis. RT Profiler PCR Arrays (SA Biosciences) are designed to determine the relative expression profile of various markers for stem cells, chemoresistance, cell proliferation, invasion, metastasis, and tumor metabolism (Fig. 2*A*). The array results were validated further by quantitative real-time PCR of selected markers (Fig. 2 *A* and *B*). The experimental results for these markers closely match the stem-cell marker data seen previously with arrays. The compilation of array results and validation data of selected markers strengthens the ovarian SP marker profile.

Differential gene expression results were examined further using computational gene network prediction tools (Ingenuity and GeneGo's MetaCore Pathway Analysis Systems) to provide a profile of key pathways for ovarian CSC function (Fig. S1*B*). In the process we identified significant up-regulation in ovarian CSCs of genes important in pluripotency, homing, and maintenance (c-Kit, Nanog, Notch, Dtx2, connexin43/Gja1, FGF1, and IGF1), self renewal (Hspa9a and Myst1/2), tumorigenic-related/angiogenic genes (EGFR family, EGFR, Her2, Erbb4, c-Met, Relb, c-Myc, Fos, and Hif1-α), chemoresistance caused by increased capacity for DNA repair (ATM and Brca2), and high multidrug transporter expression (ABCG2, MDR1, and ABCB5). We identified key stem-cell surface markers, including CD44, CD24, c-kit, CD133, and ALDH1, and key pathways such as Notch, TGF-β, IGF, EGF, FGF, and WNT/ β-catenin required for the maintenance of CSCs, further confirming that SP includes CSCs (Fig. 2 *A* and *B* and Fig. S1*B*). CD44, a key marker identified in our studies of ovarian CSCs, is a well-known adhesion molecule and membrane receptor for hyaluronan involved in cell motility and metastasis; it is also widely used for the isolation of CSCs in blood, breast, pancreas, colorectal, head and neck, and ovarian cancers (12–17). FACS sorting using

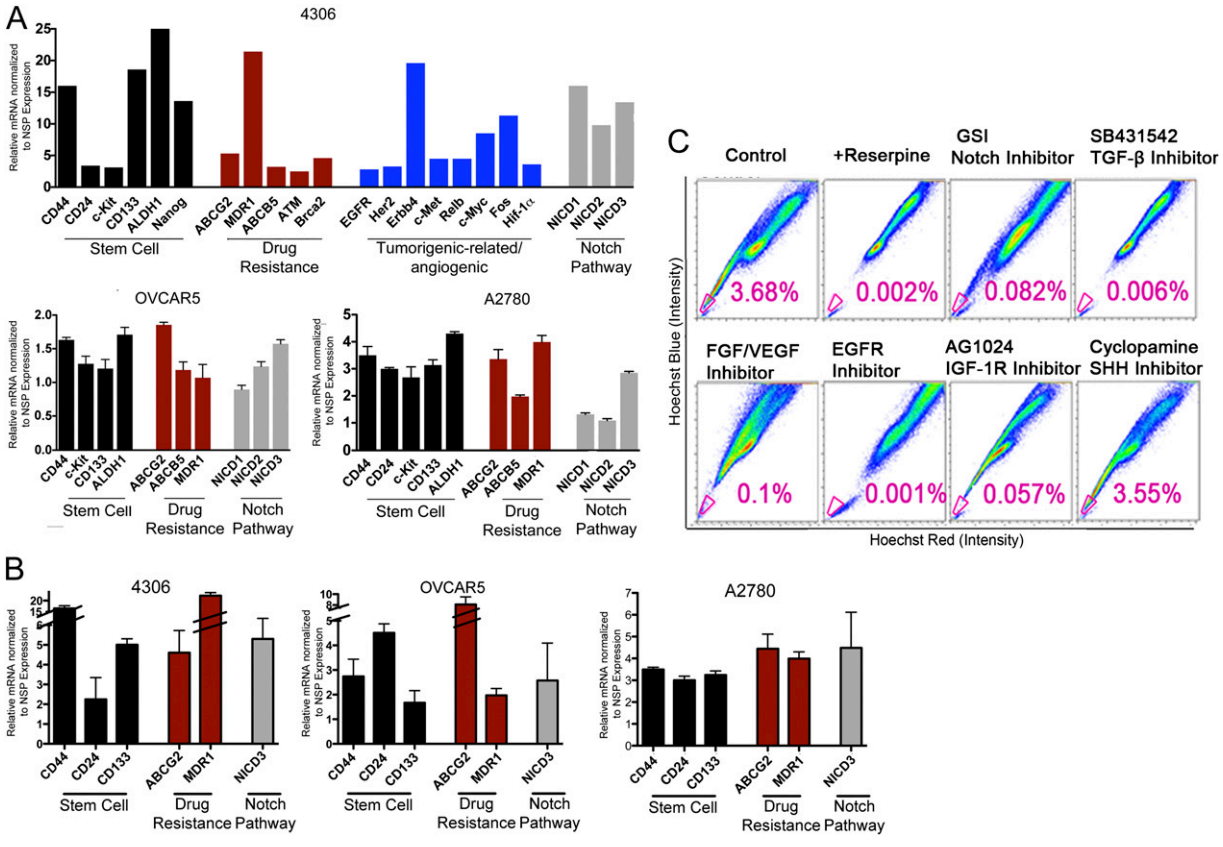

Fig. 2. Inhibition of CSC-related pathways depletes SP cells enriched for CSCs. (*A* and *B*) 4306, OVCAR5, and A2780 cells were analyzed for differential gene expression of various stem-cell and drug-resistance genes and pathways. (*C*) 4306 cells were treated with specific CSC pathway inhibitors: SB431542 (TGF-β inhibitor), PD173074 (FGF/VEGF inhibitor), AG1024 (IGF-1R inhibitor), EGFR inhibitor, GSI (Notch inhibitor), or cyclopamine (Shh inhibitor), followed by SP flow cytometry analysis. CSCs depletion is seen when using inhibitors of key CSC pathways identified by our Ingenuity and MetaCore study. Interestingly, inhibition of the Shh pathway, which was not identified by Ingenuity and GeneGo's MetaCore Pathway Analysis Systems, had no effect on CSCs. The SP percent in cells treated with Shh inhibitor was similar to that in controls.

four cell stem-cell markers, including CD44 and CD24, consistently yielded a small number of cells, especially in patient samples, which made their extensive analysis difficult. In contrast, we found SP to be an extremely reliable marker for the identification and characterization of tumor cells enriched for CSCs in a large number of experiments involving both murine and primary patient samples. As a result, we chose to use SP as a marker for the identification of therapeutics targeting the tumor population broadly enriched for CSCs rather than focusing on individual CSCs with various combinations of cell surface markers.

Using this strategy, we were able to deplete the SP population when we blocked the Notch, TGF-β, IGF, EGF, or FGF signaling pathways using specific inhibitors in vitro, suggesting that activation of these pathways is necessary for the maintenance of ovarian CSCs (Fig. 2*C*). The percent of SP was significantly lower in all the pathways tested, with the exception of the Sonic hedgehog (Shh) pathway, which was not activated in putative CSCs, validating the results obtained from the Ingenuity Analysis System (Fig. S1*B*). Interestingly, the Notch signaling pathway, which has been implicated in cell differentiation and self-renewal of stem cells, also is a key pathway for ovarian CSCs. We have found that targeting ovarian CSCs using a pan Notch pathway inhibitor, such as GSI, results in depletion of ovarian CSCs, suggesting that activation of the Notch pathway is necessary for the maintenance of CSCs. Consequently, GSI, which targets CSCs, could lead to tumor eradication in combination with cytotoxic therapies targeting the bulk of tumor cells.

To examine further the role of Notch activation in CSCs, we overexpressed the Notch1–3 intracellular domain (NICD1–3) in ovarian cancer cell lines using MigR1 retroviral vectors, which coexpress GFP with our target gene product (Fig. S1 *C* and *D*). An empty MigR1 plasmid was used to generate control cells. Overexpression of NICD was confirmed by Western blotting (Fig. 3 *A*–*C*) and real-time PCR (Fig. S1*C*). In addition, NICD overexpression resulted in increased levels for HES1, a downstream effector of Notch signaling (Fig. S1*C*). Furthermore, NICD3 overexpression was correlated with the highest increase in the levels of CD44 gene expression, a key stem-cell marker (Fig. S1*C*). The rise in CD44 levels suggests possible cross-talk between the Notch3 and CD44 signaling pathways in regulating CSCs. Indeed, when cells were analyzed for the presence of SP enriched in CSCs via flow cytometry, the percent of SP increased only in 4306 cells overexpressing NICD3 (2.36% increased to 6.53%, a 2.8-fold increase compared with control) but not in the other NICDs-transduced cells (Fig. 3*D*). This result suggests that Notch3 has a key role within the Notch signaling pathway in regulating CSCs. Furthermore, NICD overexpression conferred significant resistance to CDDP, with the highest chemoresistance seen for overexpressed Notch3 ($P < 0.001$) (Fig. 3*E*). Thus, cells with overexpressed Notch3 were 2.3 times more chemoresistant than the control cells (Fig. 3*E*). Taken together, our results indicate that the Notch pathway and Notch3 in particular are important for CSC maintenance and tumor chemoresistance to platinum. We further showed that the response to GSI is specific to the Notch pathway. FACS analysis of the SP percent in tumor cells treated with 5 or 10 μM GSI showed a dose-dependent response to GSI only in control cells but not in lines overexpressing NICD1–3 (Fig. 3*F*). This result further suggests that the effects of GSI in the maintenance of CSCs and tumor chemoresistance are indeed mediated by the Notch pathway (Fig. 3*F*). In addition, cell viability assays showed that NICD overexpression blocked the inhibitory effect of GSI (Fig. 3*G*). As expected, control cells responded to both 5- and 10-μM GSI treatments; in contrast GSI had no effect on cells overexpressing NICD1–3.

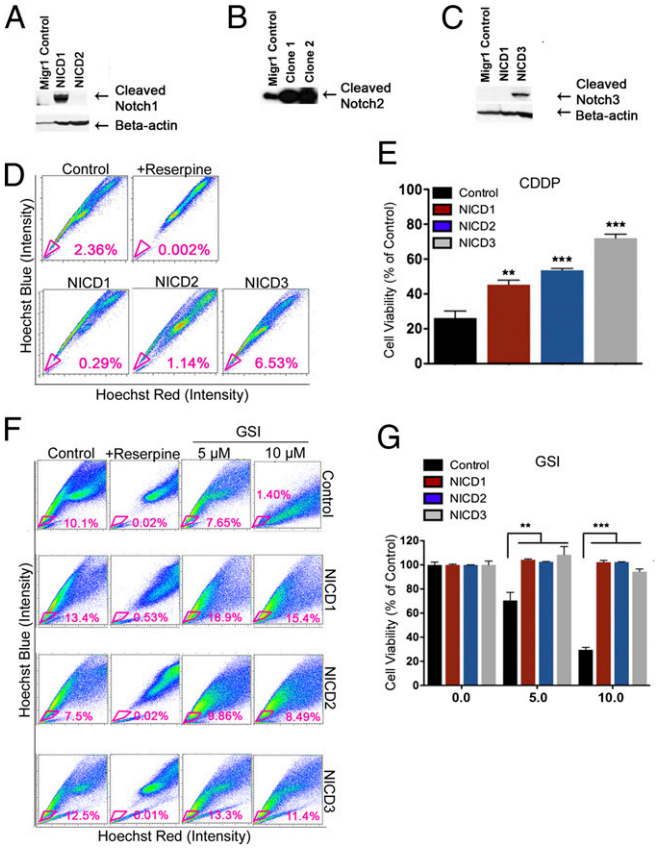

Fig. 3. Overexpression of NICD3 in 4306 cells enriches tumor CSCs and increases tumor resistance to platinum. (*A*–*C*) The intracellular domains of Notch family genes (NICD1–3) were overexpressed in 4306 murine ovarian cancer cells. Overexpression of NICD1 (*A*), NICD2 (*B*), and NICD3 (*C*) as compared with MigR1 vector control, was confirmed by Western blotting analysis. (*D* and *E*) NICD3 overexpression increased SP cell frequency (6.63%) compared with MigR1 control (2.36%) (*D*) and significantly increased tumor chemoresistance to platinum (*E*). (*F* and *G*) Notch overexpression assays confirm that GSI effects are Notch specific. Intracellular NICD overexpression rescues cells from GSI treatment. NICD1–3 overexpression blocks the reduction in SP cells (*F*) and cell viability (*G*) in response to GSI. Cells were treated with DMSO (control), 5 μM GSI, or 10 μM GSI for 48 h and then were analyzed for SP percent by FACS (*F*) Control 4306 cells showed a dose-dependent decrease in SP percent in response to 5 μM (7.65%) and 10 μM (0.37%) GSI compared with no GSI (10.1%). In contrast, the overexpressed NICD1–3 lines showed no difference in SP in response to GSI compared with control (*F*). Furthermore, when tumor cells were treated with GSI in MTT assays (*G*), control cells showed a dose-dependent decrease in cellular viability in response to 5 μM (70.48%) and 10 μM (29.56%) GSI; in contrast, GSI had no effect on cell survival (*G*) in cell lines overexpressing NICD1–3. $^{**}P < 0.01$; $^{***}P < 0.001$.

Notch Targeting by GSI Increases Tumor Sensitivity to Platinum Therapy in Vitro. Given our observation that drug-resistant CSCs were modulated by inhibition of Notch signaling, we examined whether Notch inhibitors increase tumor sensitivity to platinum therapy. Interestingly, we observed synergistic drug interactions between GSI and platinum therapy in both in vitro and in vivo studies (Fig. 4 and Figs. S2, S3, and S4; also see Fig. 6). Data collected from 3-(4,5-Dimethylthiazol-2-yl)-2,5-diphenyltetrazolium bromide (MTT) cell viability assays and tumor growth in animal models indicate a strong response to GSI and platinum and a dramatic increase in platinum sensitivity in samples from both sensitive and resistant patients. Tumor cells collected from ascites of newly diagnosed and relapsed patients were cultured in vitro. Platinum-sensitive patients were characterized by a diagnosis of clinical remission lasting longer than 6 mo after the final chemotherapy treatment. Platinum-resistant patients were defined as having relapsed within 6 mo of the final chemotherapy treatment. Refractory patients, defined by absence of a clinical response to platinum and disease progression in response to treatment, are included in the platinum-resistant group. The clinical characteristics, tumor subtype (histopathology), and sensitivity to platinum therapy for the patients included in the study are shown in Fig. S2*A*. Primary tumor cells were treated with 1 μM GSI, 10 μM CDDP, or a combination of the two treatments (Fig. 4 *A* and *B*). Mean results as assessed by

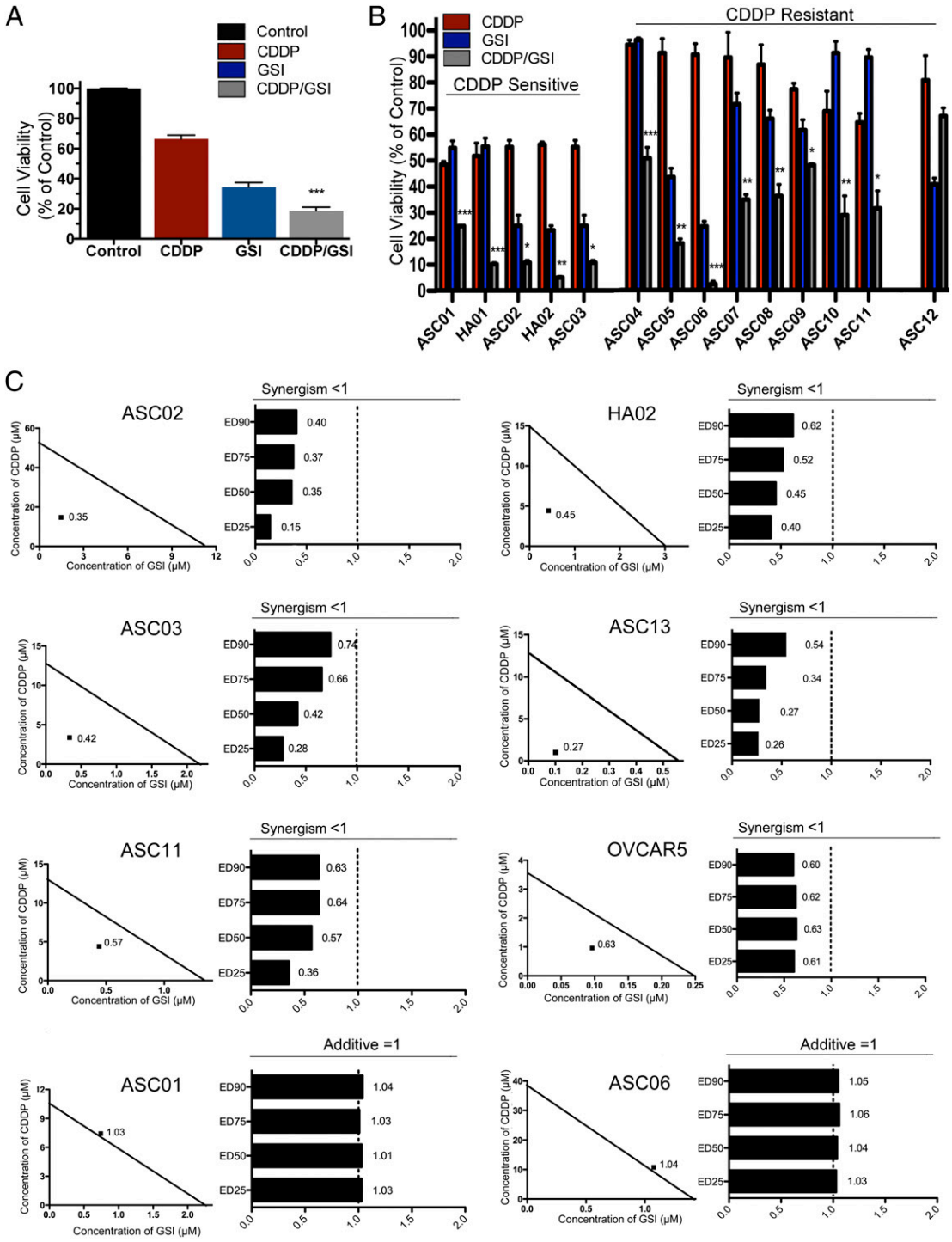

Fig. 4. MTT, isobologram, and CI analysis validates the evidence of a synergistic response to CDDP/GSI therapy in vitro. (*A* and *B*) Cells were cultured from platinum-sensitive and -resistant patients ($n = 99$) Primary tumor cells were treated with 1 μM GSI, 10 μM CDDP, or a combination of the two treatments. Mean results as assessed by MTT assays for all patient samples ($n = 99$) indicate a synergistic response to CDDP/GSI cotherapy as compared with either monotherapy (***$P < 0.001$, two-way ANOVA analysis in *A*). Cell viability in response to treatment is shown for all patients (*A*) and for individual representative platinum-sensitive and -resistant patients (*B*). Platinum-sensitive patients showed either a synergistic (ASC02, HA02, ASC03) or additive (ASC01, HA01) response to cotherapy, whereas platinum-resistant patients showed a synergistic (ASC04, ASC05, ASC07, ASC10, ASC11), additive (ASC06, ASC08, ASC09), or competitive (ASC12) response to cotherapy. The response to CDDP and to GSI monotherapy is shown in red and blue, respectively; the response to combination therapy is shown in gray. All samples showed statistical significance except for the ASC12 patient sample. *$P < 0.05$; **$P < 0.01$; ***$P < 0.001$. (*C*) Primary patient cell lines, which were analyzed previously by two-way ANOVA, were assessed further using MTT, isobologram, and CI analysis to validate the evidence of a synergistic response to GSI/CDDP therapy. Cell viability was measured by MTT assay and assessed with CalcuSyn software to provide evidence for a CDDP/GSI synergistic response in ASC02, HA02, ASC03, ASC13, and ASC11 samples (CI <1) or an additive response in ASC01 and ASC06 cells (CI = 1). Additional established cell lines (OVCAR5) were assessed using the same method. OVCAR5, which overexpresses Notch3, shows a synergistic cytotoxic response to CDDP/GSI therapy (CI <1). The CI values are shown for ED_{25}, ED_{50}, ED_{75}, and ED_{90}. The CI values provided demonstrate a synergistic effect for a wide range of CDDP and GSI effective doses.

MTT assays for all patient samples ($n = 99$) indicate a synergistic response to CDDP/GSI cotherapy compared with either monotherapy ($P < 0.001$, two-way ANOVA analysis) (Fig. 4*A*). Cell viability in response to treatment is shown for all patients (Fig. 4*A*) and for individual representative platinum-sensitive and -resistant patients (Fig. 4*B*). Platinum-sensitive patients showed either a synergistic (ASC02, HA02, ASC03) or additive (ASC01, HA01) response to cotherapy, whereas platinum-resistant patients showed a synergistic (ASC04, ASC05, ASC07, ASC10, ASC11), additive (ASC06, ASC08, ASC09), or competitive (ASC12) response to cotherapy. The synergistic response was verified in a subset of the patient population using an isobologram and combination index (CI) analysis (CalcuSyn software; Biosoft) for an extended range of CDDP (0–80 μM) and GSI (0–8 μM) concentrations (Fig. 4*C* and Fig. S2*B*). CI values were obtained for a reduction in cell viability of 25% (ED_{25}), 50% (ED_{50}), 75% (ED_{75}), and 90% (ED_{90}) and demonstrated a consistent synergistic response at all dose concentrations. Furthermore, patterns of significant reduction ($P < 0.05$, two-tailed t test) in cell viability for the combination therapy compared with CDDP monotherapy were observed across therapeutically relevant CDDP (2.5–20 μM) and GSI (0.25–2 μM) doses for all patient samples in which a synergistic or additive CDDP/GSI cotherapy response was observed (Fig. S2*B*). Synergism is indicated by CI values less than 1, whereas a CI value equal to 1 indicates an additive interaction. Most importantly, the Notch-based therapy showed great efficacy for both platinum-sensitive and -resistant patients as well as for newly diagnosed and relapsed patients. Therefore, the clinical status or platinum sensitivity of the patient does not appear to influence the efficacy of the combination therapy. Additional established cell lines (OVCAR5 and SKOV3) were assessed using MTT, isobologram, and CI analysis. Consistent with our other in vitro and in vivo findings, OVCAR5 cells, which overexpress Notch3, show a synergistic cytotoxic response to CDDP/GSI therapy (CI <1) (Fig. 4*C*). In contrast, SKOV3 tumor cells, in which Notch3 expression is not detected, demonstrate an antagonistic response to combination therapy (CI > 1) (Fig. S2*B*).

Sensitivity to GSI Is Correlated to Notch3 Expression Patterns. In light of our results using GSI therapy and recent data from the Cancer Genome Atlas (TCGA) (27) showing that Notch3 is amplified in high-grade ovarian serous carcinomas, we decided to determine how Notch3 levels affected the response of primary ovarian cancer cells to 1 μM GSI. Using cell viability MTT assays, we determined primary cell line sensitivity to GSI (Fig. 5*A*). The response to GSI for SKOV3, an established ovarian cancer cell line that lacks Notch3 expression and that has been shown to be relatively resistant to GSI (60–70% cell viability in response to GSI) by multiple groups (23, 24), including ours, was chosen as the threshold for GSI sensitivity. Patient samples deemed GSI sensitive (cell viability in response to 1 μM GSI lower than 60%) or GSI resistant (cell viability in response to 1 μM GSI higher than 60%) were analyzed by Western blotting analysis for the presence or absence of Notch3 expression (Fig. 5*A*). Interestingly, 100% of the GSI-sensitive patients showed various levels of Notch3 expression, whereas all GSI-resistant patients showed no detectable Notch3 expression.

GSI and CDDP Combination Therapy Contributes to Tumor Eradication by Effectively Targeting Both CSCs and the Bulk of Tumor Cells. To test further the effects and mechanism of action of CDDP and GSI on both SP and NSP cells, we analyzed SP and NSP percentages in OVCAR5 cells treated for 48 h with CDDP, GSI, and CDDP/GSI combination therapy by flow cytometry (Fig. 5*B*). We found that the CDDP/GSI combination enhances cell death in vitro compared with either monotherapy and is the only treatment that effectively targets both CSCs (SP) and the bulk of tumor cells (NSP). Interestingly, CDDP alone has only a minimal effect on the SP, decreasing it from 12.8 to 10.2% while effectively killing a large proportion of the bulk tumor cells (NSP decreases in CDDP-treated cells from 23.6 to 7.33%) (Fig. 5*B*). This finding corroborates our previous results suggesting that conventional chemotherapies are ineffective against CSCs. In contrast, GSI treatment specifically decreased the percent of SP from 12.8% in the control to 2.31%, which was decreased further to 0.81% when treated in conjunction with CDDP (Fig. 5*B*). Consequently, CDDP targets mostly NSP cells, whereas GSI targets Notch-dependent cells, including SP. Most importantly, the CDDP/GSI combination treatment is the only therapy that effectively eliminates both SP and NSP cells, indicating that a dual combination targeting both cancer stem cells and the bulk of tumor cells is critical for tumor eradication.

Similar to GSI, Notch3 siRNA Knockdown Increases Platinum Sensitivity, Further Demonstrating That Modulation of Tumor Chemosensitivity by GSI Is Notch Specific. Interestingly, we have found that inhibition of Notch3 activity with either siRNA or GSI sensitizes ovarian cancer cells to CDDP in tumor cell lines and patient samples that show Notch3 expression but not in lines in which Notch3 expression is absent. For these experiments we successfully used an siRNA specific for the Notch3 protein, which results in effective knockdown of Notch3 gene expression (both Santa Cruz and Sigma siRNAs were used, with similar results). PA-1 and OVCAR3 cells, which overexpress Notch3, and SKOV3 cells, in which Notch3 is absent, were transfected with a Notch3-specific siRNA and used as a negative control. Cell lines were chosen based on their basal Notch3 expression levels as determined by Western blotting analysis (Fig. 5*C*). RNA was extracted from the transfected cells and was analyzed by quantitative real-time PCR for gene expression of Notch3 and HES-1, a downstream effector of the Notch signaling pathway.

As expected, our study showed decreased expression of both Notch3 and HES-1 in PA-1 cells. In comparison with PA-1 cells transfected with a fluorescent control, expression of HES-1 and Notch3 decreased 23-fold and 37-fold, respectively (Fig. 5*D*). Similarly, HES-1 and Notch3 expression were decreased 11-fold and 28-fold, respectively, in OVCAR3 cells transfected with Notch3 siRNA as compared with OVCAR3 control cells (Fig. 5*D*). In contrast, HES-1 and Notch3 expression levels were not significantly different from the control in SKOV3 cells transfected with Notch3 siRNA or cells transduced with a scrambled siRNA negative control sequence (Fig. 5*D*). Using cell viability MTT assays, we further showed that PA-1 cells transfected with siRNA were sensitized to CDDP treatment (Fig. 5*E*). Thus, PA-1 cells transfected with Notch3 siRNA showed a significant twofold decrease in cell viability compared with control when treated with 2 μM CDDP (32.7% in siRNA transfected cells versus 62.78% detected in control PA-1 cells) (Fig. 5*E*). Similarly, OVCAR3 cells transfected with Notch3 siRNA showed improved response to platinum therapy compared with control when treated with 10 μM CDDP (Fig. 5*E*). By contrast, SKOV3 cells transfected with Notch3 siRNA and treated with 10 μM CDDP showed a cell viability of 58.21%, compared with 39.08% seen in SKOV3 control cells (Fig. 5*E*). Therefore, given that SKOV3 does not have a significant amount of Notch, the siRNA did not knock down the protein effectively or increase sensitivity to CDDP.

Treatment of Ovarian Tumors with CDDP/GSI Cotherapy Significantly Increases Platinum Response and Survival in Vivo in GEMM and Primary Tumor Xenografts. To further explore the role of the Notch pathway and CSCs in chemoresistance and disease recurrence, we used several animal models, including the K-ras/Pten/luciferase (luc) GEMM and human tumor xenografts PA-1/luc, OVCAR5/luc, and SKOV3/luc, which show varying levels of SP percent and Notch3 expression. PA-1 and OVCAR5 cells have high Notch3 expression; the K-ras/Pten GEMM model, from which we derived the 4306 and 4412 cell lines, shows low to moderate Notch3 expression; and SKOV3 cells show no detectable Notch3 expression (Fig. 5*C* and Fig. S3*A*).

We first compared the efficacy of CDDP (3 mg/kg body weight), GSI (5 mg/kg body weight), and the combination therapy in the K-ras/Pten/luc GEMM model, which develops de novo ovarian tumors that propagate intraperitoneally. Treatments were administered once every 3 d for a total of six treatments (two cycles of

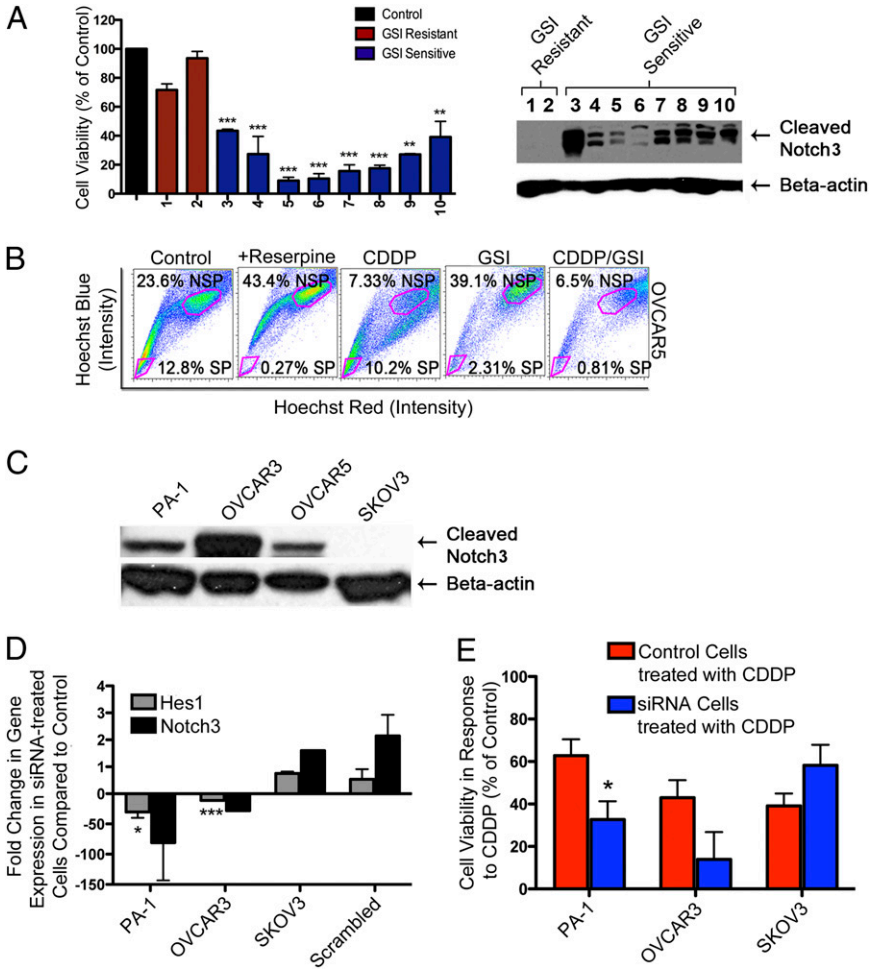

Fig. 5. Similar to GSI, down-regulation of Notch3 expression using a Notch3 siRNA knockdown strategy increases platinum sensitivity. (*A*) Western blotting analysis was carried out with lysates from GSI-resistant patients (lanes 1 and 2) and GSI-sensitive patients (lanes 3–10). Notably, lysates from GSI-sensitive patients showed overexpression of Notch3, but lysates from GSI-resistant patients showed no detectable expression of Notch3. Control response for all cell lines was averaged. The response to GSI treatment was statistically significant compared with control cells (**$P < 0.01$, ***$P < 0.001$). (*B*) OVCAR5 cells were treated with CDDP, GSI, CDDP/GSI, or DMSO (control) for 48 h and analyzed for CSC (SP) percentage. The CDDP/GSI combination is the only treatment that effectively reduces both CSCs (SP percent decreases from 12.8 to 0.81%) and the bulk of tumor cells (NSP percent decreases from 23.6 to 6.5%). CDDP treatment had a minimal effect on SP (SP percent decreases only from 12.8 to 10.2%) but depleted the majority of NSP cells (NSP percent decreases from 23.6 to 7.3%). (*C*) Notch3 was found to be overexpressed in PA-1, OVCAR3, and OVCAR5 human ovarian cancer cell lines and absent in SKOV3 when analyzed by Western blotting analysis. (*D*) HES1 and Notch3 expression levels are significantly lower in PA-1 and OVCAR3 cells transfected with Notch3 siRNA than in controls. SKOV3 cells transfected with Notch3 siRNA or cells transduced with a scrambled siRNA negative control sequence show no decrease in Notch3 or HES1. *$P < 0.05$, ***$P < 0.001$. (*E*) Notch3 knockdown increases platinum sensitivity in PA-1 and OVCAR3 cells compared with control cells. SKOV3 shows no significant change in CDDP sensitivity following Notch3 knockdown. *$P < 0.05$.

three treatments per cycle). Using the IVIS imaging system (Caliper Life Sciences Inc.), we quantified the treatment efficacy by measuring the change in bioluminescence signal compared with a pretreatment baseline (Fig. S3*B*). We observed disease stabilization in mice receiving GSI or CDDP monotherapies (mean fold change in bioluminescence 1.19 and 0.96, respectively, compared with baseline). Tumor bulk and metastases showed the greatest reduction in response to CDDP/GSI cotherapy, as indicated by bioluminescence signaling (mean fold change in bioluminescence 0.47 compared with baseline, $P < 0.001$, two-way ANOVA analysis compared with either monotherapy) (Fig. S3*B*). Furthermore, the effect of combination therapy in 50% of mice resulted in a complete response to treatment, because we found no evidence of tumor burden by palpation and imaging after treatment. These mice also showed no occurrence of relapse immediately following cessation of treatments. Conversely, disease progression resumed shortly in monotherapy groups once treatment was stopped. Survival curves revealed that, in addition to causing disease remission, the combinatorial effect of CDDP/GSI also prolonged survival significantly relative to CDDP ($P < 0.05$) or GSI ($P < 0.01$) monotherapies.

Likewise, CDDP/GSI cotherapy in tumor xenografts injected i.p. with either PA-1 or OVCAR5 tumor cells resulted in a significantly prolonged disease remission and increased survival in vivo (Fig. 6 *A* and *B*, respectively). In contrast, no increased response to CDDP/GSI therapy was seen in the SKOV3/luc mice, in which tumors do not show detectable Notch3 levels (Fig. 5*C* and Fig. S3 *A* and *C*). In the PA-1 cohort (Fig. 6*A*), we observed the expected disease progression in the control group (fold change in bioluminescence 20.7 ± 6.7 compared with baseline) and disease stabilization (mean bioluminescence fold change 1.1 ± 0.5 compared with baseline) in CDDP-treated mice. The greatest tumor response was seen in the CDDP/GSI combination group (mean bioluminescence fold change 0.19 ± 0.12 compared with baseline and a 5.8-fold significant decrease in average tumor burden compared with CDDP) (Fig. 6*A*). The response to CDDP/GSI cotherapy was significantly increased compared with CDDP ($P < 0.05$). Interestingly, although disease was stabilized initially in mice treated with CDDP, they all relapsed once treatment was discontinued. In contrast, the majority of the mice that received cotherapy showed disease remission after completion of treatment. Furthermore, the CDDP/GSI mice survived for a longer time after treatment, with most of the treated mice still alive and with no evidence of disease at the end of the experiment (Fig. 6*A*). Likewise, in the OVCAR5 cohort (Fig. 6*B*), we observed disease stabilization in CDDP (mean bioluminescence fold change 0.41 ± 0.20 compared with baseline) and GSI (mean bioluminescence fold change 0.71 ± 0.22 compared with baseline) monotherapy groups after six treatments. OVCAR5 mice showed a similar strong response after six CDDP/GSI treatments (mean bioluminescence fold change 0.06 ± 0.10 compared with baseline), resulting in eradication of tumor in four of the six mice after six treatments (Fig. 6*B*). The response to CDDP/GSI treatment was significantly greater than to either monotherapy alone (a 5.8-fold and an 11.8-fold significant decrease in average tumor burden compared with CDDP, $P < 0.01$, or GSI, $P < 0.001$, respectively). In contrast, in the SKOV3 group we did not see greater efficacy or increased survival when comparing the CDDP/GSI and CDDP groups (Fig. S3*C*). Furthermore, FACS analysis of primary cell lines developed from excised PA-1 tumors treated with CDDP demonstrate an average 3.6-fold increase in the percentage of SP cells in comparison with control

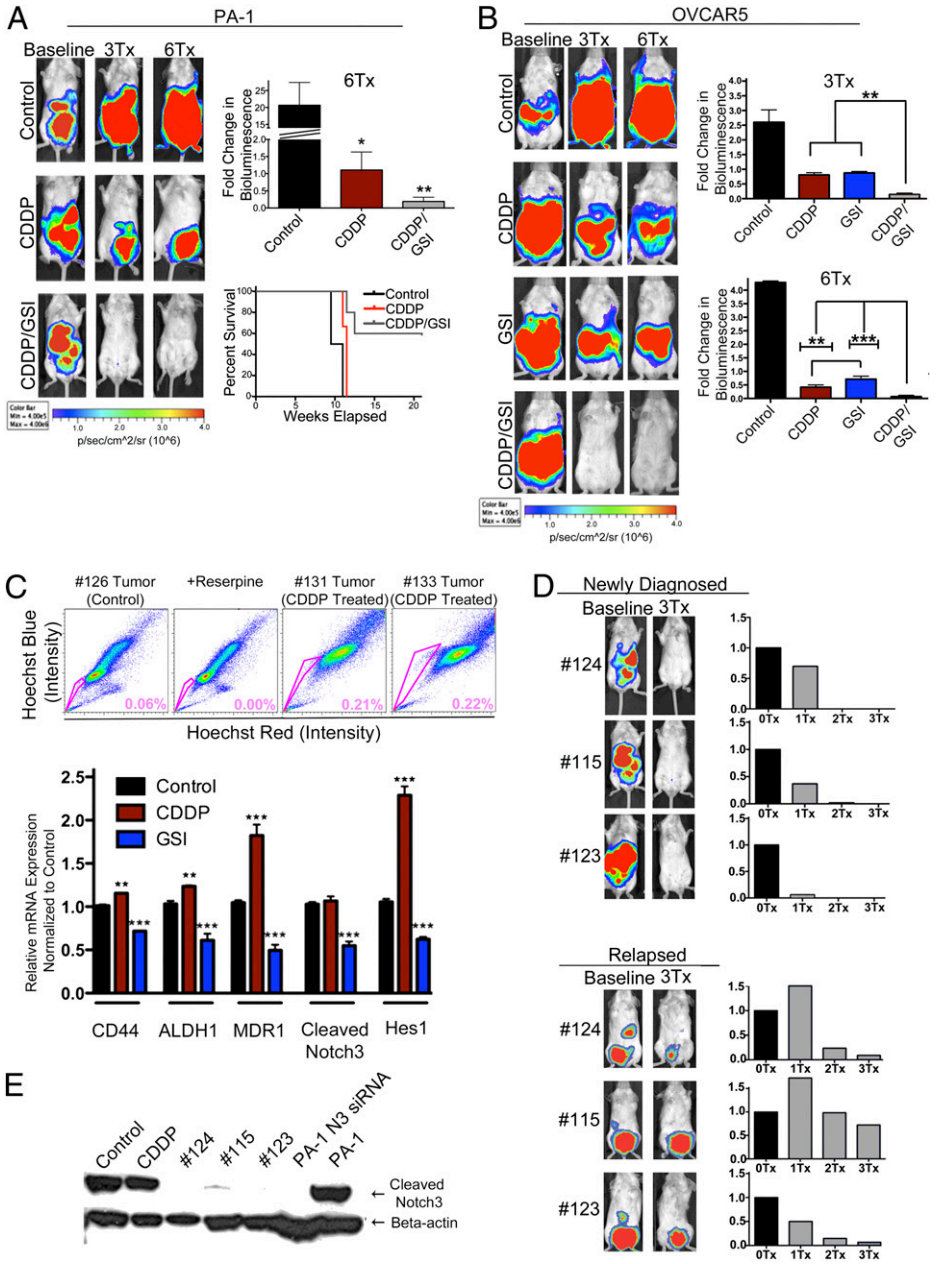

Fig. 6. Treatment of ovarian tumors with CDDP/GSI cotherapy significantly increases platinum response and survival in vivo. (*A* and *B*) Drug-efficacy studies were conducted in PA-1/luc and OVCAR5/luc tumor xenograft models. To generate all xenograft models, mice were injected i.p. with 2.5 million PA-1/luc and OVCAR5/luc cells, respectively. (*A*) Both CDDP monotherapy ($n = 6$) and CDDP/GSI cotherapy ($n = 8$) showed significant inhibition of disease progression ($^*P < 0.05$ for CDDP and $^{**}P < 0.01$ for CDDP/GSI) compared with PA-1/luc control mice ($n = 4$). CDDP/GSI-treated mice showed a statistically significant decrease in tumor burden compared with CDDP alone ($^*P < 0.05$) and is the only group that achieved long-term remission. Kaplan–Meier survival curves indicate that the combination therapy greatly enhances survival time compared with CDDP. 3Tx, mice receiving three treatments; 6Tx, mice receiving six treatments. (*B*) Similar results are seen in OVCAR5/luc-injected xenografts. In comparison with monotherapy, CDDP/GSI treatment ($n = 6$) resulted in a significant decrease in tumor burden after three treatments ($^{**}P < 0.01$ vs. CDDP, $n = 6$, or GSI, $n = 4$, respectively) and six treatments ($^{**}P < 0.01$ vs. CDDP and $^{***}P < 0.001$ vs. GSI). (*C*) FACS analysis of cell lines developed from excised tumors in PA-1 CDDP-treated mice show a 3.6-fold increase in the percent of SP cells compared with control tumor cells. Similarly, real-time PCR analysis of tumors removed from OVCAR5 mice treated with CDDP demonstrates that CDDP enriches tumors for CSCs and increases stem-cell and drug-resistant markers MDR1, CD44, and ALDH1 compared with control tumors ($^{**}P < 0.01$ for CD44 and ALDH1; $^{***}P < 0.001$ for MDR1). In contrast, GSI treatment effectively reduces the percent of CSCs and decreases the same stem-cell and drug-resistant markers MDR1, CD44, and ALDH1 ($^{***}P < 0.001$ vs. control). GSI also significantly downregulates Notch3 and HES1 levels ($^{***}P < 0.001$ vs. control), suggesting an efficient target inhibition of the Notch pathway in tumor cells. (*D*) Three mice in the PA-1 cohort (#124, 115, and 123) initially were treated successfully with CDDP/GSI cotherapy but later relapsed after a lengthy remission. Following initial diagnosis of the disease, three CDDP/GSI treatments (3Tx) successfully eradicated tumors and achieved remissions. In contrast, the relapsed tumors became less responsive to combination therapy. Quantification of tumor signals in newly diagnosed and relapsed mice indicates that newly diagnosed tumors respond to the initial treatment much more rapidly and efficiently than they do following relapse. (*E*) Western blotting analysis of tumors excised from CDDP/GSI-treated mice demonstrates complete inhibition of Notch3 by GSI in both newly diagnosed and relapsed mice. Furthermore, the inhibitory effect of GSI replicates that of a Notch3 siRNA by specifically blocking the expression of cleaved Notch3.

tumors (Fig. 6*C*). Similarly, quantitative real-time PCR analysis of tumors excised from OVCAR5 mice treated with CDDP shows significantly higher levels for stem cell surface and drug-resistance markers, including CD44, ALDH1, and MDR1 ($P < 0.01$ for CD44, ALDH1; $P < 0.001$ for MDR1). This indicates that tumor exposure to conventional platinum therapy leads to enrichment of SP cells (Fig. 6*C*). In contrast, GSI treatment significantly decreases CD44, ALDH1, and MDR1 gene-expression levels ($P < 0.001$) (Fig. 6*C*), suggesting that Notch-based therapy targets and decreases the percent of SP tumor cells. As expected, we also observed decreased levels of cleaved intracellular Notch3 and HES1 downstream effector in GSI-treated OVCAR5 tumors ($P < 0.001$) (Fig. 6*C*), further suggesting that the inhibitory GSI effects are Notch pathway specific.

To compare and contrast the difference in response to treatment between newly diagnosed and relapsed mice, we treated a cohort of PA-1 mice with CDDP/GSI cotherapy and examined the effects of therapy from initial treatment to relapse and subsequent treatment. After initial diagnosis of the disease, one cycle (three injections per cycle) of the CDDP/GSI cotherapy successfully eradicated tumors (Fig. 6*D*). After treatment was discontinued and mice achieved lengthy remissions, some of the animals (#124, 115, and 123) eventually relapsed. Relapsed mice underwent an additional cycle of therapy and were then imaged and sacrificed (Fig. 6*D*). Interestingly, they responded more slowly and less significantly to therapy than they did upon initial diagnosis (Fig. 6*D*). Excised tumors from CDDP and CDDP/GSI treated PA-1 mice were used to prepare tissue lysates for Western blotting analysis of Notch3 expression in controls and treated tumors. Although imaging still indicated significant tumor presence, no Notch3 expression was detected in Western blots of tumors treated

with CDDP/GSI cotherapy. As a positive control, PA-1 and PA-1 cells transfected with Notch3 siRNA also were analyzed. Normal PA-1 cells showed high Notch3 protein levels, whereas PA-1 cells transfected with Notch3 siRNA showed no Notch3 expression. This finding demonstrates that GSI effects are Notch specific, given that the results of an efficient Notch3 knockdown with siRNA are virtually identical to those seen with GSI (Fig. 6*E*). Despite effective blocking of the Notch signaling pathway by GSI, animals that suffered a relapse could not achieve a long-term remission. Consequently, relapsed tumor cells, including CSCs, no longer were completely dependent on the Notch signaling pathway; additional signaling pathways provided input and were responsible for the failure to achieve remission. Therefore, our data suggest that Notch inhibitors should be added to the first line of platinum treatment to achieve the best results therapeutically.

CDDP/GSI Cotherapy Enhances the DNA-Damage Response, G_2/M Cell-Cycle Arrest, and Cell Death. In addition to reducing the percent of CSCs, GSI was found to act synergistically with CDDP in Notch-dependent tumor cells to enhance the DNA damage, cell-cycle arrest, and apoptotic response. We chose OVCAR5 cells to test the extent of DNA damage induced by CDDP and GSI because it has shown high Notch3 expression (Fig. S4*A*). We treated cells with 5μM CDDP, 1μM GSI, or a combination therapy, respectively, for 4 h and determined by immunofluorescence (IF) the number of γ-H2AX foci, a sensitive marker of DNA damage (Fig. S4 *B* and *C*). Both CDDP and GSI were effective in initiating DNA damage after 4 h. Interestingly, tumor exposure to the CDDP/GSI combination therapy increased the number of γ-H2AX foci compared with either monotherapy. Quantification of IF data showed that DNA damage induced by CDDP/GSI combination therapy in OVCAR5 cells was increased significantly ($P < 0.001$ by two-way ANOVA analysis) compared with either monotherapy (Fig. S4 *B* and *C*). In contrast, SKOV3 cells, which do not express Notch3, showed no significant difference between DNA-damage responses to CDDP/GSI and CDDP treatments (Fig. S4 *B* and *C*). To substantiate our findings that GSI potentiates the DNA-damage response and apoptosis induced by CDDP, we performed a cell-cycle analysis using propidium iodide staining of the same OVCAR5 and SKOV3 cell lines. Cells were treated with 5 μM CDDP, 1 μM GSI, or a combination therapy for 24 h before staining. Previous work has shown that CDDP arrests cells in G_2/M and induces apoptosis (28–30). We found that GSI significantly potentiated the cell-cycle arrest in G_2/M induced by CDDP in OVCAR5 cells ($P < 0.001$, two-way ANOVA) (Fig. S4*D*); the percentage of cells arrested in G_2/M was significantly higher in response to CDDP/GSI combination treatment than to either monotherapy. In contrast, no significant increase in the G_2/M cell-cycle arrest was observed in SKOV3 cells (Fig. S4*D*). Furthermore, we performed a Western blotting analysis of poly(ADP-ribose) polymerase (PARP) cleavage, a well-characterized apoptotic marker, to assess the levels of apoptosis that occur in OVCAR5 and SKOV3 cells treated with CDDP/GSI cotherapy versus monotherapy. Accumulation of PARP cleavage was found to be significantly greater in OVCAR5 cells treated with CDDP/GSI combination treatment than in cells treated with either monotherapy ($P < 0.001$, two-way factorial ANOVA) (Fig. S4*E*), but this difference was not significant when CDDP/GSI therapy was compared with CDDP in SKOV3 cells (Fig. S4*E*). These results assess multiple aspects of the cell-death response induced by the CDDP/GSI combination treatment and support the addition of a Notch inhibitor to platinum therapy clinically. Combined, these data corroborate our previous in vitro and in vivo results indicating that GSI and CDDP cooperate to induce an enhanced DNA-damage response, a G_2/M cell-cycle arrest, and increased cell death in Notch-dependent tumor cells.

Discussion

Standard chemotherapy in ovarian cancer results in tumor cytoreduction but infrequently results in a cure. It is well established that CSCs have key characteristics allowing them to survive standard cancer chemotherapy and radiation therapy. Our data and results of recent studies indicate that CSCs are a major source of tumor development and resistance to chemotherapy (5–17). We and others have demonstrated that SP cells are more tumorigenic and chemoresistant than NSP cells (12–17, 31). We confirmed the CSC characteristics of SP cells by establishing a transcriptional molecular profile of sorted ovarian cancer SP. In addition to stemness-related genes, we also identified several tumorigenic and angiogenesis-related, drug-resistance, and key pathways for stem cells, including Notch, in SP cells. The increased expression of these proto-oncogenes in ovarian cancer has been associated with aggressive tumor behavior, advanced disease stage, and poor prognosis. Interestingly, our study indicates that ovarian CSCs express high levels of CD44 and drug transporters (MDR1, ABCG2, ABCB5), DNA repair genes (ATM, Brca2), and genes associated with platinum resistance, such as Connexin43/Gja1, and Cyp1a1. Up-regulation of ATP-binding cassette transporters within CSCs is likely a major mechanism that contributes to the acquisition of multidrug chemoresistance. Indeed, we have shown that ovarian CSCs show an inherently high chemoresistance to platinum. We also have demonstrated that CSCs expand during acquisition of platinum chemoresistance.

Notch is a conserved pathway that has been implicated in the maintenance of tissue homeostasis by regulation of self-renewal and cell-fate determination in normal stem cells and early progenitors. Recent studies, including TCGA data, have found that the Notch pathway is misregulated in ovarian cancer (23–25, 27, 32–33). In addition, Notch3 gene copy number is increased and correlates with aggressive tumor behavior and poor prognosis in ovarian serous adenocarcinomas (23–25, 27, 32–33). Interestingly, we now have data showing that the Notch signaling pathway, and Notch3 in particular, plays a key role in CSC maintenance and platinum chemoresistance. Thus, our results indicate that when we blocked the Notch pathway using GSI, a pan-Notch inhibitor, we observed a significant depletion in SP cells, further validating our hypothesis that the activation of Notch is necessary for the maintenance of ovarian CSCs. In addition, our data indicate that when the Notch signaling pathway is constitutively activated via overexpression of NICDs, specifically NICD3, SP cell frequency increased several fold. Similarly, we found that cell lines in which NICD1–3, and especially NICD3, were overexpressed were more resistant to CDDP treatment. Furthermore, inhibition of Notch3 activity with either siRNA or GSI sensitizes ovarian cancer cells to CDDP in tumor cell lines and in patient samples exhibiting high levels of Notch3 expression but not in lines in which Notch3 is absent. Park et al. (32) determined that Notch3 expression is higher in recurrent tumors than in primary samples, providing further evidence that Notch3 signaling is a factor contributing to the development of tumor chemoresistance and disease relapse. Our results strongly suggest that the Notch3 signaling pathway is important for CSC maintenance and tumor resistance to platinum. The effects of GSI in depleting CSCs and sensitizing tumors to platinum therapy are Notch pathway specific, given that NICD1-3 overexpression rescues cells from GSI action. Thus, GSI had no effect on cell viability or on the percent of SP cells in cell lines in which NICD1–3 is overexpressed.

Furthermore, we have observed synergistic drug interactions between GSI and platinum therapy in both in vitro and in vivo studies. Interestingly, sensitivity to GSI was correlated with the presence or absence of Notch3 gene expression in a panel of samples from GSI-sensitive and -resistant patients. This observation may become important in clinical studies, because it will allow us to identify the patients who would benefit most from GSI treatment based on their Notch3 expression levels. Our analysis of primary patient samples shows that CDDP and GSI cotherapy has a synergistic cytotoxic effect compared with CDDP or GSI monotherapies in both platinum-resistant and -sensitive patient groups. Furthermore, the CDDP/GSI combination treatment is the only therapy that effectively eliminates both SP and NSP cells, indicating that a dual combination targeting both CSCs and the

bulk of tumor cells is critical for tumor eradication. Our in vivo data from both GEMM and human tumor xenografts with various levels of Notch3 expression support this observation. GSI sensitizes cells to CDDP action and allows CDDP to reduce tumor burden more effectively and prolong disease-free survival in tumor cells dependent on Notch signaling, including CSCs.

It is well known that platinum-based drugs, such as CDDP, cause DNA damage (28–30, 34). Both cisplatin and carboplatin induce DNA damage, primarily at guanine residues, generating monoadducts and interstrand crosslinks leading to inhibition of DNA replication, transcription, and ultimately to cell death (28–30, 34). In our study, we examined the effect of Notch pathway inhibition by GSI on DNA damage by observing the phosphorylation of histone γ-H2AX foci. The combination therapy significantly increased the effects of DNA damage, G_2/M cell-cycle arrest, and apoptosis compared with either monotherapy. These results further confirm our observation that GSI increases the efficacy of platinum therapy by sensitizing cells to CDDP-induced DNA damage and enhancing the rate of tumor cell death. Based on our results, we believe that inhibition of the Notch pathway with GSI or an equivalent inhibitor could be a highly effective strategy in overcoming platinum chemoresistance in a clinical setting.

Long-term survival of ovarian cancer patients is poor due to high rates of therapeutic failure and tumor relapse. Patient stratification based on individual genetic make-up and the addition of a front-line therapeutic agent specifically targeting CSCs to the first line of therapy have the potential to result in more effective therapies for ovarian cancer patients. Discovering reliable chemosensitivity markers and assays that could predict clinical outcome accurately is critical. In future studies we plan to identify Notch transcriptional signatures using both patient and murine samples. Such analysis will allow us to identify markers of clinical interest to assess the response to Notch therapy in vivo; these markers could be of great use in clinical trials using GSI or Notch-selective inhibitory antibodies. Recently, multiple studies have described Notch-selective inhibitory antibodies that specifically inhibit individual Notch receptors by blocking their negative regulatory domains (35). Intestinal toxicity, which is mentioned as a secondary effect for GSI therapy in some patients, likely will be avoided when using a Notch3-selective antibody (35). We anticipate that this work will pave the way in the near future for a clinical trial to evaluate the efficacy of selective anti-Notch antibodies, such as anti-Notch3, in enhancing the response to platinum treatment.

Materials and Methods

Additional experimental details are included in *SI Materials and Methods*.

Notch Overexpression and Knockdown Studies. We employed both gain-of-function and loss-of-function strategies to assess the contribution of the Notch pathway to CSC function and platinum chemoresistance. NICD1-3 intracellular domains were overexpressed in 4306 ovarian cancer cells. Additionally, we used siRNAs to downregulate Notch3 gene expression in human PA-1 and OVCAR3 cell lines, which overexpress Notch3, and SKOV3, in which no Notch3 is detected (negative control). FACS analysis and MTT cell viability assays were used to assess the percentage of SP cells and response to CDDP.

Statistical Analysis. Dose-response curves were analyzed using Prism (GraphPad) and CalcuSyn software packages. Statistical significance of in vitro and in vivo assay results was determined using univariate two-tailed t-tests, one-way ANOVA, and two-way factorial ANOVA tests. The isobologram and CI analysis was performed using the dose effect analysis software (CalcuSyn). All data were expressed as means ± standard error. A $P < 0.05$ was considered statistically significant.

ACKNOWLEDGMENTS. This work was supported by Department of Defense Ovarian Cancer Research Program Award W81XWH-10-1-0263 (D.M.D.), a V Foundation Scholar Award (D.M.D.), an Ovarian Cancer Research Fund Liz Tilberis Award (D.M.D.), by Burroughs Wellcome (D.M.D.), by the Mary Kay Ash (D.M.D.) and Rivkin Foundations (D.M.D.), and by a generous contribution from the Mildred Moorman Ovarian Cancer Research Fund (D.M.D.).

1. Permuth-Wey J, Sellers TA (2009) Epidemiology of ovarian cancer. *Methods Mol Biol* 472:413–437.
2. Cannistra SA (2004) Cancer of the ovary. *N Engl J Med* 351:2519–2529.
3. Ozols RF, et al. (2004) Focus on epithelial ovarian cancer. *Cancer Cell* 5:19–24.
4. Auersperg N, Wong AS, Choi KC, Kang SK, Leung PC (2001) Ovarian surface epithelium: Biology, endocrinology, and pathology. *Endocr Rev* 22:255–288.
5. Reya T, Morrison SJ, Clarke MF, Weissman IL (2001) Stem cells, cancer, and cancer stem cells. *Nature* 414:105–111.
6. Campbell LL, Polyak K (2007) Breast tumor heterogeneity: Cancer stem cells or clonal evolution? *Cell Cycle* 6:2332–2338.
7. Shackleton M, Quintana E, Fearon ER, Morrison SJ (2009) Heterogeneity in cancer: Cancer stem cells versus clonal evolution. *Cell* 138:822–829.
8. Shipitsin M, et al. (2007) Molecular definition of breast tumor heterogeneity. *Cancer Cell* 11:259–273.
9. Mani SA, et al. (2008) The epithelial-mesenchymal transition generates cells with properties of stem cells. *Cell* 133:704–715.
10. Marotta LL, Polyak K (2009) Cancer stem cells: A model in the making. *Curr Opin Genet Dev* 19:44–50.
11. Polyak K, Hahn WC (2006) Roots and stems: Stem cells in cancer. *Nat Med* 12:296–300.
12. Szotek PP, et al. (2006) Ovarian cancer side population defines cells with stem cell-like characteristics and Mullerian Inhibiting Substance responsiveness. *Proc Natl Acad Sci USA* 103:11154–11159.
13. Alvero AB, et al. (2009) Molecular phenotyping of human ovarian cancer stem cells unravels the mechanisms for repair and chemoresistance. *Cell Cycle* 8:158–166.
14. Moserle L, et al. (2008) The side population of ovarian cancer cells is a primary target of IFN-alpha antitumor effects. *Cancer Res* 68:5658–5668.
15. Zhang S, et al. (2008) Identification and characterization of ovarian cancer-initiating cells from primary human tumors. *Cancer Res* 68:4311–4320.
16. Wei X, et al. (2010) Mullerian inhibiting substance preferentially inhibits stem/progenitors in human ovarian cancer cell lines compared with chemotherapeutics. *Proc Natl Acad Sci USA* 107:18874–18879.
17. Meirelles K, et al. (2012) Human ovarian cancer stem/progenitor cells are stimulated by doxorubicin but inhibited by Mullerian inhibiting substance. *Proc Natl Acad Sci USA* 109:2358–2363.
18. Bookman MA, et al. (1996) Carboplatin and paclitaxel in ovarian carcinoma: A phase I study of the Gynecologic Oncology Group. *J Clin Oncol* 14:1895–1902.
19. McGuire WP, et al. (1996) Cyclophosphamide and cisplatin compared with paclitaxel and cisplatin in patients with stage III and stage IV ovarian cancer. *N Engl J Med* 334:1–6.
20. Armstrong DK, et al.Gynecologic Oncology Group (2006) Intraperitoneal cisplatin and paclitaxel in ovarian cancer. *N Engl J Med* 354:34–43.
21. Walker JL, et al. (2006) Intraperitoneal catheter outcomes in a phase III trial of intravenous versus intraperitoneal chemotherapy in optimal stage III ovarian and primary peritoneal cancer: A Gynecologic Oncology Group Study. *Gynecol Oncol* 100:27–32.
22. Gupta PB, et al. (2009) Identification of selective inhibitors of cancer stem cells by high-throughput screening. *Cell* 138:645–659.
23. Choi JH, et al. (2008) Jagged-1 and Notch3 juxtacrine loop regulates ovarian tumor growth and adhesion. *Cancer Res* 68:5716–5723.
24. Park JT, et al. (2006) Notch3 gene amplification in ovarian cancer. *Cancer Res* 66:6312–6318.
25. Shih IeM, Wang TL (2007) Notch signaling, gamma-secretase inhibitors, and cancer therapy. *Cancer Res* 67:1879–1882.
26. Dinulescu DM, et al. (2005) Role of K-ras and Pten in the development of mouse models of endometriosis and endometrioid ovarian cancer. *Nat Med* 11:63–70.
27. Cancer Genome Atlas Research Network (2011) Integrated genomic analyses of ovarian carcinoma. *Nature* 474:609–615.
28. Sorenson CM, Barry MA, Eastman A (1990) Analysis of events associated with cell cycle arrest at G2 phase and cell death induced by cisplatin. *J Natl Cancer Inst* 82:749–755.
29. Nicioli da Silva G, et al. (2010) Cell cycle arrest and apoptosis in TP53 subtypes of bladder carcinoma cell lines treated with cisplatin and gemcitabine. *Exp Biol Med* 235:814–824.
30. Wang S, et al. (2012) Molecular imaging of p53 signal pathway in lung cancer cell cycle arrest induced by cisplatin. *Mol Carcinog*, 10.1002/mc.21930.
31. Hosonuma S, et al. (2011) Clinical significance of side population in ovarian cancer cells. *Hum Cell* 24:9–12.
32. Park JT, et al. (2010) Notch3 overexpression is related to the recurrence of ovarian cancer and confers resistance to carboplatin. *Am J Pathol* 177:1087–1094.
33. Matulonis UA, et al. (2011) High throughput interrogation of somatic mutations in high grade serous cancer of the ovary. *PLoS ONE* 6:e24433.
34. Cruet-Hennequart S, et al. (2009) Characterization of the effects of cisplatin and carboplatin on cell cycle progression and DNA damage response activation in DNA polymerase eta-deficient human cells. *Cell Cycle* 8:3039–3050.
35. Wu Y, et al. (2010) Therapeutic antibody targeting of individual Notch receptors. *Nature* 464:1052–1057.